

G. Beaulieu and D. Noiseux

Institut de Recherche d'Hydro-Québec (IREQ)  
1800 Mtée Ste-Julie  
Varenes, Québec, Canada, JOL 2P0

ABSTRACT

The numerical solution of the coupled differential equations of motion of the blades of an horizontal axis wind turbine is a more direct approach than the technique of finite elements, permitting the optimization of the design at relatively low cost. The procedure consists in transforming the equation of motion into a set of first order equations and solving them with fourth order Runge-Kutta integrators. This technique is applied to a twisted, tapered blade of variable cross section and stiffness including discontinuities. The first six natural frequencies and mode shapes are obtained.

This technique is extended to obtain the polar moment of inertia of the blades as a function of frequency and rotational speed.

A good match with the experimental results is achieved.

INTRODUCTION

The accurate determination of natural frequencies is of fundamental importance in the design of wind turbine blades. Similarly, the polar moment of inertia of the blades is required for the study of the torsional dynamics of the drive train.

Rotor dynamics is often studied with the use of large and specialized finite elements computer codes. However, the availability and cost of operation of these programs limit their use, and a more direct approach could be beneficial. The direct solution of the coupled differential equations of motion of the blade is such an approach, permitting optimization studies at low cost. This paper presents a model of a nonuniform, tapered, twisted cantilever wind turbine blade and a method of solution.

For the purpose of demonstrating the method, only the in-plane and out-of-plane bending modes are considered since the torsional modes occur at frequencies much higher than the bending modes because of the high torsional rigidity of the blade. The coupled differential equations of motion were transformed into a set of first order equations and solved with Runge-Kutta numerical integrators. The turbine blade under study has major stiffness discontinuities. The blade is therefore considered as if made of adjoining segments, each one having a varying stiffness.

The first and second derivatives of the stiffness curves evidently have to be considered. The continuity of the shear forces and moments was imposed between each segments of the blade. With these variations of the Runge-Kutta method it is possible to obtain the resonant frequencies and the normalized distributions of displacement, bending moment and shear force for the first six bending modes. The coriolis forces and the tension force due to centrifugal loading are included. The modes of vibration are computed for a regime of rotational speed. The normal and tangential aerodynamic loading at each section of the blade could be included as extra terms in the differential equations; however, this paper considers only a rotor turning without the aerody-

amic forces. These will be included in further studies dealing with the optimization of small capacity wind turbines.

An important extension to this model consists in the formulation of the polar moment of inertia of the rotor in terms of a couple at a frequency  $\omega$  applied to the hub and the resultant angular acceleration of the rotor. A direct method using the shear forces and moments produced by each blade at the hub and an integral from using the in-plane displacements (mode shape) along the blades are formulated and the numerical results compared. The polar moment of inertia is then obtained as a function of frequency and rotational speed.

THE EQUATIONS OF MOTION AND THE TRANSFORMATION METHOD

Lets consider a turbine blade turning outside the aerodynamic and gravity field with its main axis perpendicular to the rotation axis mounted as a cantilever into a rigid hub. The tension in the blade due to centrifugal loading is included. If the blade elongation is assumed to be small relative to the transversal displacements, it can be demonstrated that the coriolis forces become negligible. When only the in-plane and out-of-plane bending motions are considered, the coupled differential equations become:

$$\frac{\partial^2}{\partial z^2} \left[ EI_{xy} \frac{\partial^2 v}{\partial z^2} + EI_{yy} \frac{\partial^2 u}{\partial z^2} \right] - \frac{\partial}{\partial z} \left[ T \frac{\partial u}{\partial z} \right] = m \omega^2 u \tag{1a}$$

$$\frac{\partial^2}{\partial z^2} \left[ EI_{xy} \frac{\partial^2 u}{\partial z^2} + EI_{xx} \frac{\partial^2 v}{\partial z^2} \right] - \frac{\partial}{\partial z} \left[ T \frac{\partial v}{\partial z} \right] = m (\omega^2 + \Omega_0^2) v \tag{1b}$$

These equations are a subset of the equations of Houbolt and Brooks (ref. 1) and an extension of the equations of Canergie and Dawson (ref. 2) for a twisted blade. In these equations, the tension

T at any section of the blade is independent of the vibration frequency  $\omega$  but proportional to  $\Omega_0^2$  and represented by:

$$T = \Omega_0^2 \int_z^L m(z) z dz \quad (2)$$

Taking the first and second derivatives of the terms in bracket while considering the moments of inertia  $I_{xx}$ ,  $I_{yy}$  and  $I_{xy}$  as variable along the z axis, the system of equation (1) becomes:

$$\begin{aligned} EI_{yy} u^{IV} + EI_{xy} v^{IV} = -E \left[ 2 I'_{xy} v''' + 2 I'_{yy} u''' \right. \\ \left. + I''_{xy} v'' + I''_{yy} u'' \right] + Tu'' + T'u' \\ + m\omega^2 u \end{aligned} \quad (3a)$$

$$\begin{aligned} EI_{xy} u^{IV} + EI_{xx} v^{IV} = -E \left[ 2I'_{xy} u''' + 2 I'_{xx} v''' \right. \\ \left. + I''_{xy} u'' + I''_{xx} v'' \right] + Tv'' + T'v' \\ + m \left( \omega^2 + \Omega_0^2 \right) v \end{aligned} \quad (3b)$$

where ( )' and ( )''... indicate the first, second, ..., derivatives with respect to z. It is seen from these equations that the in-plane and out-of-plane bending are coupled through  $I_{xy}$  and its first derivative  $I'_{xy}$ .

The method of transformation of variables, first proposed by Canergie and Dawson (ref. 2) is generalized by applying it at any frequency of vibration and not exclusively to find the resonant frequency. The two fourth order equations are transformed into eight first order equations by the following substitutions:

$$\begin{aligned} Y_1 = v''' & & Y_5 = v' \\ Y_2 = u''' & & Y_6 = u' \\ Y_3 = v'' & & Y_7 = v \\ Y_4 = u'' & & Y_8 = u \end{aligned} \quad (4)$$

By substitution and differentiation the following eight first order equations are obtained:

$$\begin{aligned} EI_{xy} Y_1' + EI_{yy} Y_2' = -E \left[ 2I'_{xy} Y_1 + I''_{xy} Y_3 \right. \\ \left. + 2 I'_{yy} Y_2 + I''_{yy} Y_4 \right] + T Y_4 + T' Y_6 \\ + m\omega^2 Y_8 \end{aligned} \quad (5a)$$

$$\begin{aligned} EI_{xx} Y_1' + EI_{xy} Y_2' = -E \left[ 2 I'_{xy} Y_2 \right. \\ \left. + I''_{xy} Y_4 + 2 I'_{xx} Y_1 + I''_{xx} Y_3 \right] \\ + T Y_3 + T' Y_5 + m \left( \omega^2 + \Omega_0^2 \right) Y_7 \end{aligned} \quad (5b)$$

$$Y_3' = Y_1 \quad (5c)$$

$$Y_4' = Y_2 \quad (5d)$$

$$Y_5' = Y_3 \quad (5e)$$

$$Y_6' = Y_4 \quad (5f)$$

$$Y_7' = Y_5 \quad (5g)$$

$$Y_8' = Y_6 \quad (5h)$$

They can be conveniently represented by:

$$\begin{aligned} Y_i' = f_i(z, Y_1, Y_2, \dots, Y_8) \\ i = 1, 2, \dots, 8 \end{aligned} \quad (6)$$

Applying the appropriate boundary conditions, it is then possible to solve equation (6) with the use of Runge-Kutta numerical integrators.

The displacements and their first, second and third derivatives are then obtained. From these, one can compute the distributions of the shear forces and moments by the usual relations:

$$\begin{aligned} F_x = -E \left[ I_{xy} v''' + I'_{xy} v'' + I_{yy} u''' \right. \\ \left. + I'_{yy} u'' \right] + Tu' \end{aligned} \quad (7a)$$

$$\begin{aligned} F_y = -E \left[ I_{xy} u''' + I'_{xy} u'' + I_{xx} v''' \right. \\ \left. + I'_{xx} v'' \right] + Tv' \end{aligned} \quad (7b)$$

$$M_x = E \left[ I_{xy} v'' + I_{yy} u'' \right] \quad (7c)$$

$$M_y = E \left[ I_{xy} u'' + I_{xx} v'' \right] \quad (7d)$$

#### THE BOUNDARY CONDITIONS

Consider the turbine blade shown in figure 1. The longitudinal axis of the blade is the z axis and the rotor turns in the y-z plane. The x axis is the axis of rotation. The blade is mounted in a rigid hub at 6% of its span ( $\ell$ ) and has a total length of 4.95 meters (L).

Because the blade is rigidly mounted the boundary conditions are:

$$u = v = u' = v' = 0 \text{ at } z = \ell$$

$$\text{that is } Y_i(\ell) = 0 \text{ for } i = 5, 6, 7, 8 \quad (8)$$

At the free end the conditions are:

$$u'' = v'' = u''' = v''' = 0 \text{ at } z = L$$

since the moments and shear forces are zero; that is  $Y_i(L) = 0$  for  $i = 1, 2, 3, 4$  (9)

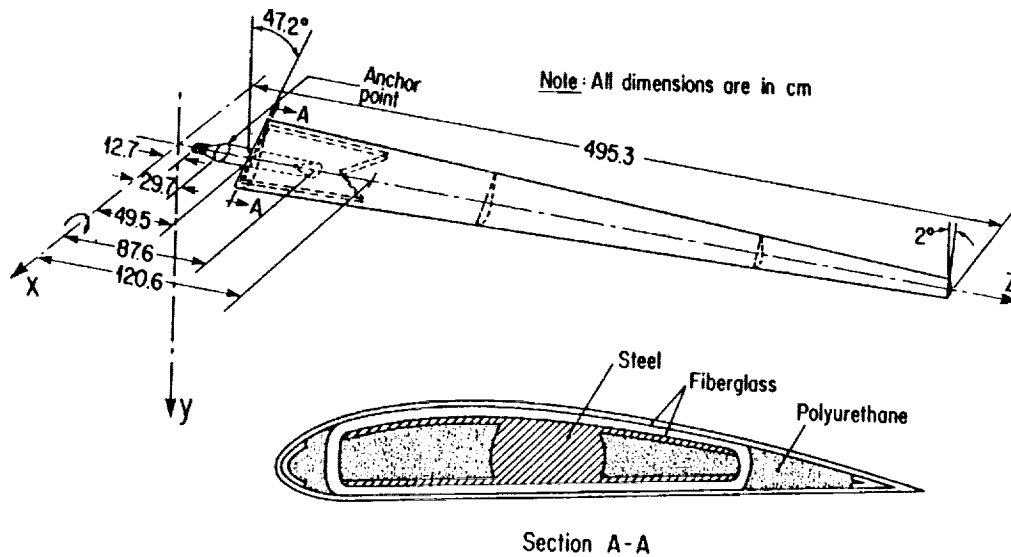


Figure 1 - Geometry of IREQ turbine blade

These boundary conditions apply to a stationary blade. When the hub is allowed to rotate around the x axis the conditions at the free end remain unchanged but the displacement  $v$  and its slope  $v'$  are different from zero at  $z = \ell$ . However,  $u$  and  $u'$  remain zero since the hub is assumed rigid. Therefore, if the rotor is allowed to spin and oscillate in the plane of rotation the boundary conditions at  $z = \ell$  become:

$$\begin{aligned} u &= u' = 0 \\ v &= v(\ell) \\ v' &= v'(\ell)/\ell \end{aligned} \quad (10)$$

This last condition is the consequence of the rigid hub being displaced by an amount  $v(\ell)$  at  $\ell$ .

#### THE METHOD OF SOLUTION

The method of solving equation (5) is as follows:

- 1) A value is selected for the frequency  $\omega$ ;
- 2) The four known boundary conditions (equation 7) at the root are set and the four unknown conditions are given arbitrary values namely:

$$Y_1 = C_0, Y_2 = Y_3 = Y_4 = 0 \quad (11)$$

- 3) From these eight boundary conditions at the root a solution is obtained with the use of fourth order Runge-Kutta integrators. Eight values,  $Y_1$  to  $Y_8$ , are obtained for the free end:

$$\begin{aligned} Y_{i,r}(L) &= F_{i,1} \quad (i = 1, 2, \dots, 8) \\ (r = 1) \end{aligned} \quad (12)$$

where the subscript  $r = 1$  indicates the solution with the first group of boundary conditions;

- 4) Step (3) is repeated by successively setting each of the unknown boundary condition to the arbitrary value  $C_0$ . In this way four sets of starting boundary conditions are obtained for  $z = \ell$ :

	$Y_8$	$Y_7$	$Y_6$	$Y_5$	$Y_4$	$Y_3$	$Y_2$	$Y_1$
(r) case	$u$	$v$	$u'$	$v'$	$u''$	$v''$	$u'''$	$v'''$
1	0	0	0	0	$C_0$	0	0	0
2	0	0	0	0	0	$C_0$	0	0
3	0	0	0	0	0	0	$C_0$	0
4	0	0	0	0	0	0	0	$C_0$

giving four sets of solutions for the free end:

$$\begin{aligned} Y_{i,r} &= F_{i,r} \quad (i = 1, 2, \dots, 8) \\ (r = 1, \dots, 4) \end{aligned} \quad (14)$$

- 5) The solution of equation (6) is a combination of these four solutions. Namely,

$$\begin{aligned} Y_i(z) &= \sum_{r=1}^4 a_r Y_{i,r}(z) \\ (i = 1, 2, \dots, 8) \end{aligned} \quad (15)$$

However, the known boundary conditions at the free end are for a cantilever blade:

$$Y_i(L) = 0 \quad (i = 1, 2, 3, 4) \quad (16)$$

since the shear forces and moments must be zero. The right hand side of equation (15) can then be partitioned:

$$\sum_{r=1}^4 a_r F_{i,r} = 0 \quad (i = 1,2,3,4) \quad (17)$$

- 6) A non-trivial solution is possible if the determinant of the coefficients  $F_{i,r}$  of equation (17) is equal to zero

$$\begin{aligned} \left\| F_{i,r} \right\| &= 0 \quad (i = 1,2,3,4) \\ (r = 1,2,3,4) \end{aligned} \quad (18)$$

Therefore, the above steps are repeated with increased values of the vibration frequency  $\omega$  until equation (18) is satisfied. That  $\omega$  then corresponds to a resonant frequency.

- 7) Having found the resonant frequency  $a_1$  is set to 1 and  $a_2, a_3$  and  $a_4$  are computed giving the four unknown boundary conditions at the anchor point.
- 8) The solution is repeated once more with the following initial conditions:

$$\begin{aligned} Y_1 &= a_1 & Y_5 &= 0 \\ Y_2 &= a_2 & Y_6 &= 0 \\ Y_3 &= a_3 & Y_7 &= 0 \\ Y_4 &= a_4 & Y_8 &= 0 \end{aligned} \quad (19)$$

In addition to the displacement  $u$  &  $v$  the shear forces and moments are computed at each blade station with equations (7a) to (7d).

The method described above was first used by Canergie and Dawson (ref. 2) to find the natural frequencies of a straight constant section blade. Its application here is extended to twisted, tapered blade having discontinuity of rigidity.

#### TURBINE BLADE CHARACTERISTICS

The turbine blade used on the 40 kW, 10 meters IREQ wind turbine is a twisted, tapered composite blade made principally of steel and fiberglass. Figure 1 shows its construction. Its asymmetric aerodynamic profile is NACA 4415. The chord is 44.45 cm at the root and 10.92 cm at the free end with a thickness varying from 7.11 cm to 1.78 cm. The twist angle  $\beta$  goes from 47.2 degrees to 2 degrees at the tip.

The principal moments of inertia  $I_{xx_s}$  and  $I_{yy_s}$  for a group of typical blade sections were computed from an engineering drawing of the blade and were transformed into the blade principal axis (in-plane and out-of-plane) by the usual relations:

$$\begin{aligned} I_{xx} &= I_{xx_s} \cos^2 \beta + I_{yy_s} \sin^2 \beta \\ I_{yy} &= I_{yy_s} \cos^2 \beta + I_{xx_s} \sin^2 \beta \end{aligned}$$

#### BLADE CHARACTERISTICS

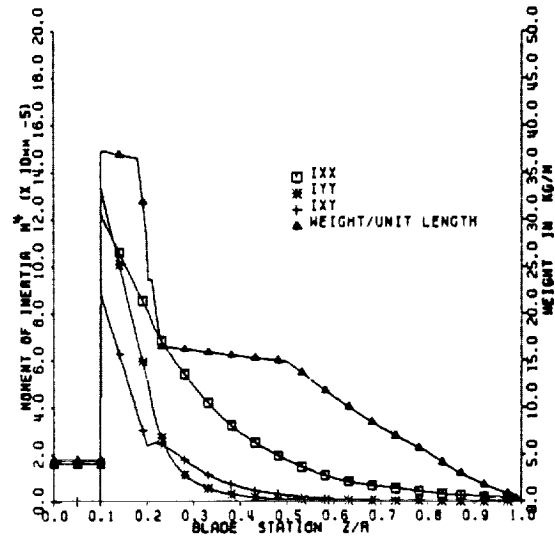


Figure 2 - IREQ turbine blade characteristics

$$I_{xy} = \frac{(I_{xx_s} - I_{yy_s})}{2} \sin 2\beta$$

The  $I_{xx_s}$  and  $I_{yy_s}$  for each element of the blade section are equivalent moment of inertia based on the same reference modulus of elasticity  $E$ . The blade actual geometry was found to be significantly different from the drawing geometry. The moment of inertia  $I_{xx_s}$  and  $I_{yy_s}$  are then corrected to account for these manufacturing inaccuracies. The values used as input to the modal analysis program are shown in figure 2. The root sections of the blade is approximated by linear distributions while the all fiberglass section from the end of the steel insert to the blade tip was approximated by a polynomial computed from twelve input data points. The first and second derivatives of  $I_{xx}$ ,  $I_{yy}$  and  $I_{xy}$  were numerically computed from the above distributions.

In order to take care of the discontinuities of stiffness, the blade is divided into three sections, the first from the anchor point to the blade root section, the second up to the end of the steel insert and the third to the tip of the blade.

The numerical integration is done from the anchor point to the tip of the blade in a continuous manner except that the values of four of the eight state variables ( $Y_1$  to  $Y_4$ ) are varied in a stepwise manner at the two major discontinuities of the blade. This is done because the state variables being integrated at each segment of the blade are the numerical derivatives of the displacements  $u$  and  $v$ , namely  $u', v', u'', v'', u'''$  and  $v'''$  and not the forces and moments in the blade. The physical quantities that must be continuous are the displacements, the slopes, the moments and the shear forces and the tension, not the derivatives. Therefore the continuity of the boundary conditions become:

$$\begin{aligned}
u_- &= u_+ & M_{x_-} &= M_{x_+} \\
u'_- &= u'_+ & M_{y_-} &= M_{y_+} \\
v_- &= v_+ & F_{x_-} &= F_{x_+} \\
v'_- &= v'_+ & F_{y_-} &= F_{y_+} \\
T_- &= T_+
\end{aligned}
\tag{20}$$

The indices - and + represent the sections immediately to the left and immediately to the right of the discontinuity. Using equation (7a) to (7d) and equation (20), it is possible to find new values (the + values) for the derivatives  $u''$ ,  $v''$ ,  $u'''$ , and  $v'''$  that will ensure the continuities of the forces and moments across the discontinuity. Performing the appropriate algebra on equations (7) and (20), we get:

$$u''_+ = \frac{\begin{bmatrix} M_{y_-} & M_{x_-} & I_{xx_+} \\ E & -EI_{xy_+} & \end{bmatrix}}{\begin{bmatrix} I_{xx_+} & I_{yy_+} \\ I_{xy_+} & -I_{xy_+} \end{bmatrix}}
\tag{21a}$$

$$v''_+ = \frac{\begin{bmatrix} M_{y_-} & -I_{xy_+} u''_+ \\ EI_{xx_+} & -I_{xx_+} \end{bmatrix}}{\begin{bmatrix} I_{xx_+} & I_{yy_+} \\ I_{xy_+} & -I_{xy_+} \end{bmatrix}}
\tag{21b}$$

$$u'''_+ = \frac{\begin{bmatrix} \left( -\frac{F_{y_-}}{E} - I'_{xy_+} u''_+ - I'_{xx_+} v''_+ + \frac{T_+}{E} v'_+ \right) - \frac{I_{xx_+}}{I_{xy_+}} \\ \left( -\frac{F_{x_-}}{E} - I'_{yy_+} v''_+ - I'_{xy_+} u''_+ + v''_+ + \frac{T_+}{E} u'_+ \right) \end{bmatrix}}{\begin{bmatrix} I_{xx_+} & I_{yy_+} \\ I_{xy_+} & -I_{xy_+} \end{bmatrix}}
\tag{21c}$$

$$\begin{aligned}
v'''_+ &= \frac{1}{I_{xy_+}} \left[ -\frac{F_{x_-}}{E} - I'_{yy_+} u''_+ - I'_{xy_+} v''_+ \right. \\
&\quad \left. + \frac{T_+}{E} u'_+ - I_{yy_+} u'''_+ \right]
\end{aligned}
\tag{21d}$$

It is clear that the shear forces and bending moments computed with this method are not exact in the immediate region of the discontinuities. However the distribution should not be affected in regions farther from the discontinuities.

#### FORMULATION OF THE POLAR MOMENT OF INERTIA

The polar moment of inertia  $J$  of an horizontal axis wind turbine rotor is required for the analysis of the dynamic torsional stability of the drive train.  $J$  varies with the vibration frequency  $\omega$  and the rotational speed  $\Omega_0$ . The

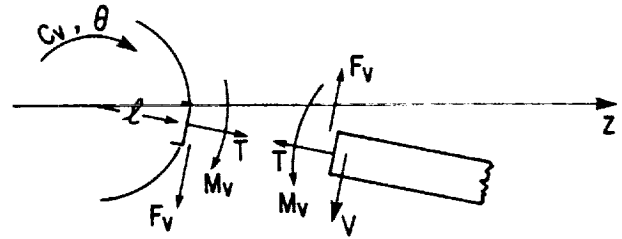


Figure 3 - Internal forces and moments at the blade anchor point.

variations of  $J$  are mainly caused by the transverse vibration of the blades. The polar moment of inertia of the rotor, excluding the hub, is defined at a frequency  $\omega$  by:

$$J = \frac{C_v}{-\omega^2 \theta}$$

where  $C_v$  is the amplitude of the couple applied by the hub at the frequency  $\omega$  and  $-\omega^2 \theta$  is the angular acceleration of the hub. For a symmetrical three bladed rotor,  $J$  will be three times the polar moment of inertia of one blade computed with respect to the rotor hub.

When a blade vibrates at a frequency  $\omega$ , an internal shear force and moment appear at the anchor point as shown in figure 3. The shear force and moment produced by the out-of-plane vibrations are reacted upon by the rigid hub and do not appear in the formulation of  $J$ . However, the hub is free to rotate around its axis and the in-plane vibrations will be reacted by the rotor hub in the form of a couple. The sign convention shown in figure 4 is introduced such that  $F_v = -\partial M / \partial z$ . The external couple  $C_v$ , applied by the hub is then:

$$C_v = -F_v(\ell) \ell - M_v(\ell)
\tag{23}$$

The tension  $T$ , being purely radial at the hub, does not produce any couple. The external couple expressed by equation (23) is then introduced in equation (22) to give:

$$J = \frac{-F_v(\ell) \ell - M_v(\ell)}{-\omega^2 v(\ell) / \ell}
\tag{24}$$

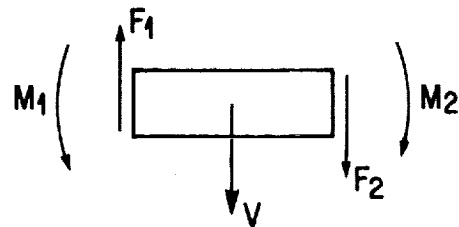


Figure 4 - Positive directions of shear forces and moments

Since T is radial at  $l$ ,  $F(l)$  and  $M(l)$  become:

$$F_v(l) = \left[ -\frac{\partial}{\partial z} \left( EI_{xx} v'' + EI_{xy} u'' \right) \right]_{z=l} \quad (25)$$

$$M_v(l) = \left[ EI_{xx} v'' + EI_{xy} u'' \right]_{z=l} \quad (26)$$

If the blade section is uniform and symmetric at the anchor point (a circular section for the IREQ blade) we have:

$$I'_{xx}(l) = I'_{xy}(l) = I'_{yy}(l) = 0 \quad (27)$$

and (25) and (26) become:

$$F_v(l) = -EI_{xx}(l) v'''(l) \quad (28)$$

$$M_v(l) = EI_{xx}(l) v''(l) \quad (29)$$

giving

$$J = \frac{EI_{xx}(l) [v''(l) - lv'''(l)]}{\omega^2 v(l)/l} \quad (30)$$

In this last equation, the polar moment of inertia of one blade is expressed in terms of the forces and moments at the rotor hub.

Another representation of the polar moment of inertia is possible if one considers the in-plane displacements of the blade as it vibrates at a frequency  $\omega$ . By using integration by parts on equations (1) and (7) and applying the appropriate boundary conditions, it can be demonstrated that

$$J = \frac{l}{v(l)} \int_l^L m v z dz \quad (31)$$

At a very low frequency, the blade is not deformed and moves as a rigid body;  $v(z)$  becomes a straight line

$$v(z) = v(l) z/l \quad (32)$$

and (31) takes the well known form of the static moment of inertia:

$$J_0 = \int_l^L m z^2 dz \quad (33)$$

Both equations (30) and (31) can be used to compute the polar moment of inertia but the integral formulation is inherently more exact from the numerical point of view because it only uses the blade in-plane displacements while equation (30) uses in addition the second and third derivatives of these displacements at the hub anchor point.

In order to compute the polar moment of inertia, the equations of motion of the blade must be

solved in the manner described above except that a value is chosen for  $\omega$  and the arbitrary value  $C_4$  used as initial condition for  $Y_1 (v''')$  is varied until the determinant (equation 18) becomes zero. When a solution is obtained for that  $\omega$ , equations (30) and (31) are used to compute  $J$ . This procedure must be repeated for each value of  $\omega$  with the following boundary conditions at  $z = l$ :

	$Y_8$	$Y_7$	$Y_6$	$Y_5$	$Y_4$	$Y_3$	$Y_2$	$Y_1$
$r$ (case)	$u$	$v$	$u'$	$v'$	$u''$	$v''$	$u'''$	$v'''$
1	o	$C_0$	o	$C_0/l$	$C_1$	o	o	o
2	o	$C_0$	o	$C_0/l$	o	$C_2$	o	o
3	o	$C_0$	o	$C_0/l$	o	o	$C_3$	o
4	o	$C_0$	o	$C_0/l$	o	o	o	$C_4$

These boundary conditions were explained earlier.

#### NUMERICAL RESULTS FOR THE MODES OF VIBRATION

The natural modes of vibration for the IREQ HAWT blade have been computed for the following conditions:

- 1) The first six modes of a stationary cantilever blade.
- 2) The first six modes of a cantilever blade at 100, 200 and 300 RPM.

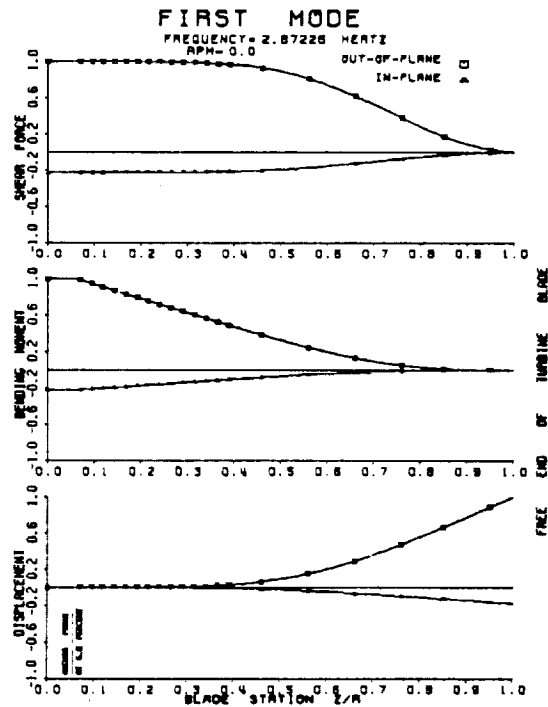


Figure 5 - First out-of-plane mode

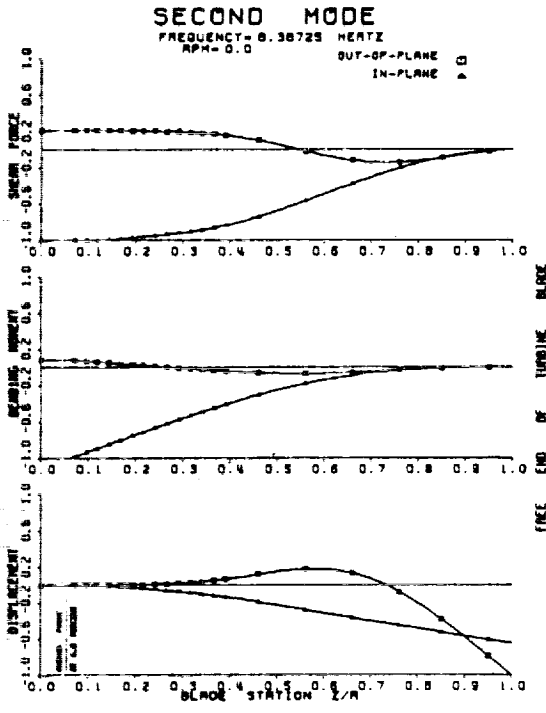


Figure 6 - Second out-of-plane mode

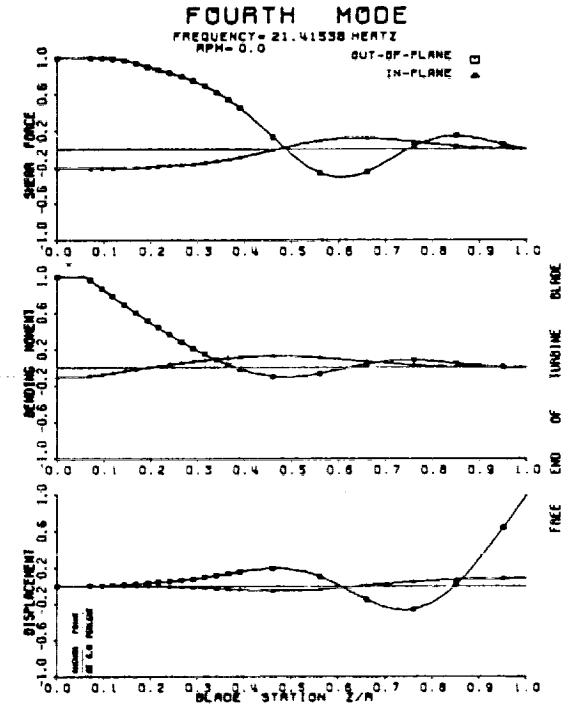


Figure 8 - Third out-of-plane mode

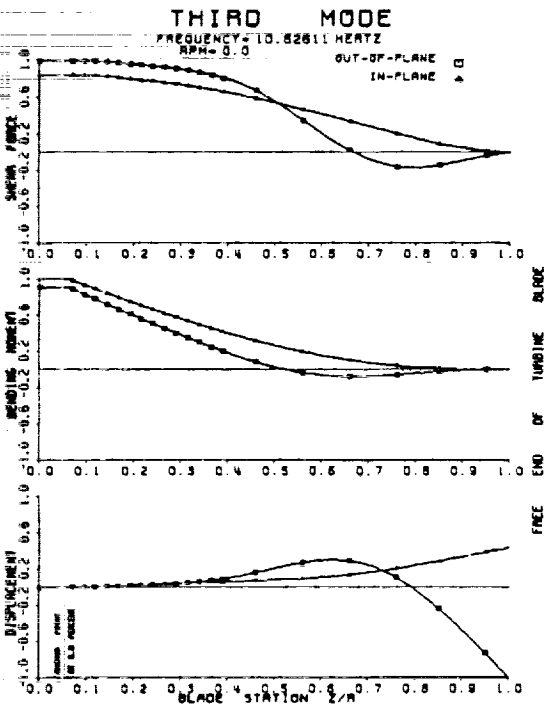


Figure 7 - First in-plane mode

For each of these cases, the following has been obtained:

- 1) The resonant frequencies (pôles). The zeros are also available from the polar moment of inertia curves.
- 2) The normalized in-plane and out-of-plane displacement curves or mode shape.
- 3) The normalized in-plane and out-of-plane shear force and bending moment distribution curves.

The results presented here are valid only for a blade mounted perpendicularly in a rigid hub. Only the coupled in-plane and out-of-plane bending modes are considered, torsion being neglected. One blade was tested experimentally in the laboratory for the stationary case only. The analytical and experimental frequencies are compared in table I.

MODES	ANALYTICAL	EXPERIMENTAL
1	2.872	2.80
2	8.387	8.00
3	10.627	10.99
4	21.415	18.66
5	31.384	27.39
6	37.474	30.77

Table I. Natural resonant frequencies in Hertz for a stationary blade.

It can be seen that the natural frequencies are in close agreement for the first few modes. The larger discrepancies for the higher modes are believed to be caused by some uncertainty in the construction causing local variations of mass and stiffness which would affect mostly the higher modes. Also, the fact that the blade support was not perfectly rigid, means that the observed frequencies would be lower than the one predicted under the cantilever assumption. Finally, the excitation of the blade was done with an electromagnetic exciter which requires some attachment hardware at the tip of the blade. This addition of mass at the tip, also tends to lower the frequencies.

The normalized mode shapes, shear forces and bending moments distribution curves are shown in figures 5 to 10 for a stationary blade. Coupling between the in-plane and out-of-plane modes is evident from the figures. It should be noted that the blade stiffness discontinuities at blade station 0.10 and 0.22 do not affect the continuity of the distribution of the bending moment and of the shear force.

The same computations were done for a rotating blade at 100, 200 and 300 RPM. Table II shows

MODE	RPM = 0	RPM = 100	RPM = 200	RPM = 300
1	2.872	3.728	5.421	7.183
2	8.387	8.649	9.099	9.594
3	10.626	11.228	13.031	15.703
4	21.415	22.143	24.161	27.117
5	31.384	31.593	32.206	33.143
6	37.474	38.206	40.246	43.486

Table II. Resonant frequencies of a rotating blade.

the resonance frequencies obtained. The effect of the rotational speed on the resonance frequencies for the three first modes is shown in figure 11. The agreement with some experimental results is good.

#### NUMERICAL RESULTS FOR THE POLAR MOMENT OF INERTIA

The polar moment of inertia of a three bladed rotor has been computed for vibration frequencies up to 70 radians/sec and rotational speed up to 200 RPM. The values of  $J_F + M$  obtained with the formula using the shear force and moment (equation 30) and the values  $J_f$  obtained with the integral formula (equation 31) give comparable results. However, as mentioned earlier the values of  $J_f$  are implicitly more accurate than the values of  $J_F + M$ . This fact is demonstrated numerically by observing that at very low frequencies, the value of  $J_f$  remains constant for all RPM used while the value of  $J_F + M$  shows small variations for each rotational speed considered.

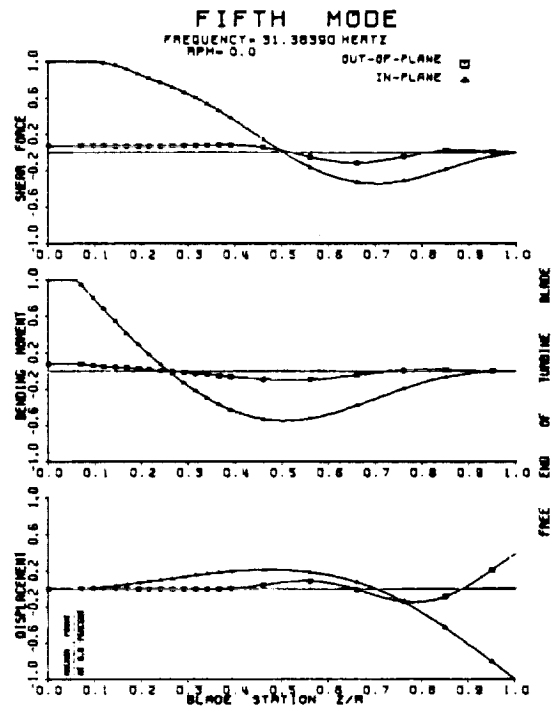


Figure 9 - Second in-plane mode

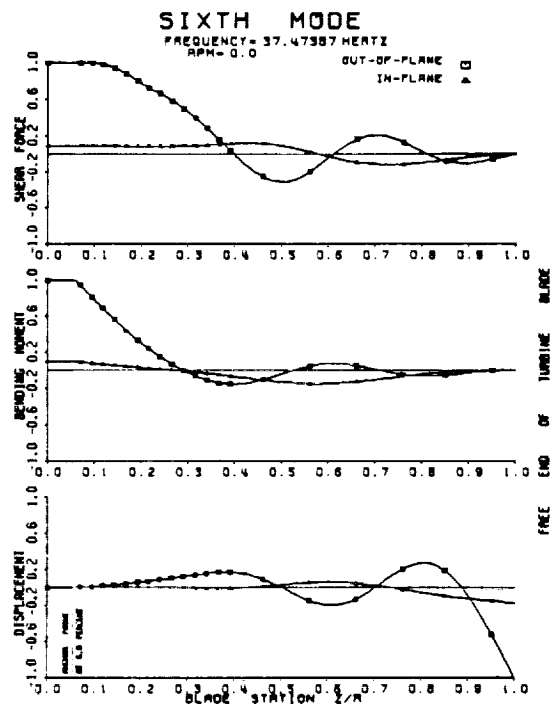


Figure 10 - Fourth out-of-plane mode

**ANALYTICAL AND EXPERIMENTAL  
VIBRATION FREQUENCIES**

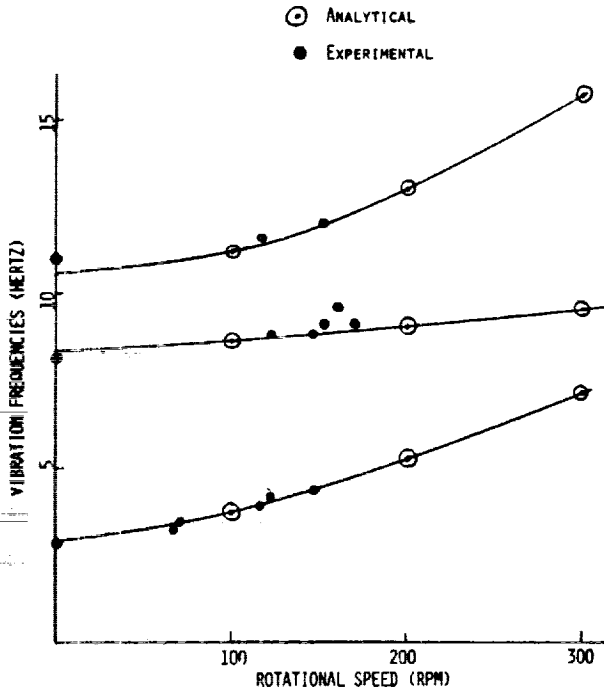


Figure 11 - Effect of rotational speed on vibration frequencies

**POLAR MOMENT OF INERTIA OF ROTOR**

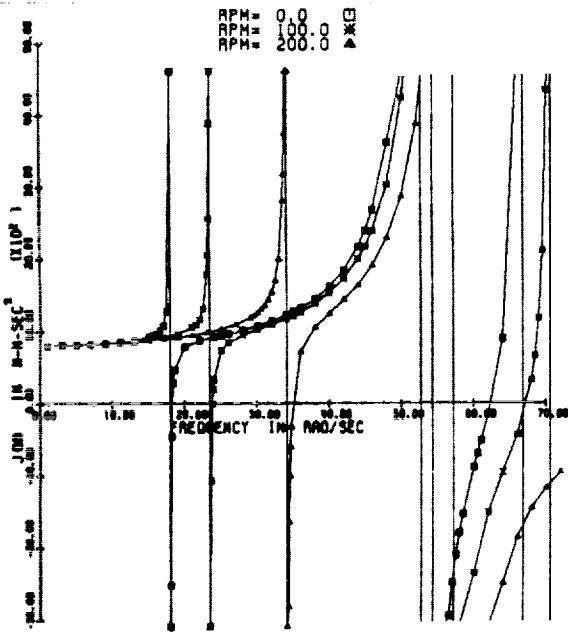


Figure 12 - Variation of polar moment of inertia in function of vibration frequency and rotational speed

The variation of the polar moment of inertia with the vibration frequency and rotational speed is presented in figure 12. Only the values of  $J_f$  are shown. The poles (resonant frequencies) and the zeros can be seen on this graph. The numerical value of the zeros are presented in table III.

ZEROS	RPM = 0	RPM = 100	RPM = 200
1	2.916	3.789	5.588
2	9.912	10.689	-

Table III. Zeros of the rotor in Hertz

It can be seen that the value of  $J$  is relatively constant at low frequency and comparable (less than 0.47% at  $\omega = 0.5$  rad/sec) to the static value  $J_0$ . (The static value  $J_0$  is 807.29 newton-meter-sec<sup>2</sup>.)

If damping had been included in the equations the extreme variations of  $J$  at a pole would be reduced, especially when a zero is very close to a pole, as is the case for the first mode. With damping the pole-zero doublet would produce only a small variation in  $J$ , its importance depending on the separation between the pole and the zero.

**CONCLUDING REMARKS**

A mathematical model and its method of solution have been presented for a tapered twisted, cantilever wind turbine blade with discontinuous stiffness. The two fourth order differential equations representing the in-plane and the out-of-plane motion of the blade have been transformed into eight first order equations and solved with Runge-Kutta integrators. The blade discontinuities have been approximated by imposing the continuity of displacements, slopes, bending moments and shear forces. The centrifugal force is included in the model; the coriolis force was found to be negligible. The polar moment of inertia of a three bladed rotor is formulated considering either the in-plane bending moment and shear force at the anchor point or the integral of the in-plane displacements for vibrating, rotating blades.

It has been demonstrated that the method is sufficient to compute the natural frequencies and mode shapes of a stationary or rotating wind turbine blade with large discontinuities in stiffness. The normalized distributions of bending moment and shear force are also computed. The polar moment of inertia has been computed as a function of frequency and rotational speed. Good agreement with experimental frequencies has been observed.

The computer program can be used efficiently for the structural optimisation of the blades of horizontal axis wind turbine. The computer time and memory requirements are relatively small (approximately 20 sec and 200 K with an IBM 370, for each mode) so that parametric studies are possible.

NOTE:

Numerical results of vibration frequencies and mode shapes for discontinuous turbine blades published by Lang and Nemat - Nasser (ref. 3) became known to us just recently, after the analysis presented here was completed. The accuracy of the method proposed here will be compared later with the results of reference 3.

ACKNOWLEDGMENT

The authors acknowledge the assistance of Bernard Saulnier, Ahmad Jamaledine, Michel Gauthier, Yvan Sunderland and Dorien Marois, all of IREQ, for the experimental data.

REFERENCES

1. Houbolt, J.C., Brooks, G.W.: Differential Equations of Motion for Combined Flapwise Bending, Chordwise Bending and Torsion of Twisted Nonuniform Rotor Blades. NACA Report 1236, 1958.
2. Canergie W., Dawson B. Vibration Characteristics of Straight Blades of Asymmetrical Aerofoil Cross-Section. The Aeronautical Quarterly, May 69, pp. 178-190.
3. Lang K.W., Nemat-Nasser S.: An Approach for Estimating Vibration Characteristics of Non-uniform Rotor Blades. AIAA Journal, Vol. 17, No. 9, Sept. 79, pp. 995-1002.
4. Shampine L.F., Watts H.H.: Comparing Error Estimators for Runge-Kutta Methods. Mathematics of Computation, Vol. 25, No. 115, July 71.
5. Hull D.G.: Fourth-Order Runge-Kutta Integrations With Stepwise Control, AIAA Journal, Vol. 15, No. 10, October 77, pp. 1505-1507.

NOMENCLATURE

$a_T$	=	Coefficients in numerical solution
$C_0, C_1, \dots, C_4$	=	Arbitrary constants used in numerical solution
$C_V$	=	Couple applied by hub at anchor point of the blade
$E$	=	Young's modulus
$F_x, F_y$	=	Shear forces in x and y directions
$I_{xx}$	=	Moment of inertia of blade about x axis
$I_{yy}$	=	Moment of inertia of blade about y axis
$I_{xy}$	=	Product of inertia
$L$	=	Total length of blade
$l$	=	Distance between axis of rotation and anchor point of the blade
$M_x, M_y$	=	Bending moments about x and y axis
$m$	=	Mass of blade per unit length
RPM	=	Rotational speed in rev/min
$T$	=	Tension force in blade
$u$	=	Displacement along x axis
$v$	=	Displacement along y axis
$x, y, z$	=	Cartesian coordinates
$Y_1, \dots, Y_8$	=	Variables of transformation
$\beta$	=	Twist angle of blade
$\theta$	=	Angular displacement of rotor
$\Omega_0$	=	Rotational speed of rotor
$\omega$	=	Vibration frequency
$( )'$	=	First derivative with respect to z
$( )''$	=	Second derivative with respect to z
$( )'''$	=	Third derivative with respect to z
$( )''''$	=	Fourth derivative with respect to z

QUESTIONS AND ANSWERS

G. Beaulieu

From: W.C. Walton

Q: Would you agree that the root support stiffness should affect the lower modes first so that this is probably not the explanation for higher mode errors?

A: *True. The support stiffness could explain the lower frequency in the first few modes, while unknown mass and stiffness distribution and the tip mass addition of the electromagnetic exciter could explain the deviations for the higher modes.*

From: W.N. Sullivan

Q: How were the experimental resonant frequencies shown measured on the turning rotor?

A: *Directly measured from strain gages recording on strip charts. We would have preferred magnetic tape recording and spectral analysis.*

From: A. Wright

Q: Why do the boundary conditions for edgewise displacements change if hub is free to rotate?

A: *When the hub is free to rotate, an in-plane displacement  $v(l)$  is present at the anchor point and similarly the slope of this displacement is  $v(l)/l$ . If the hub would be fixed,  $v$  and  $v'$  would equal zero.*

From: Y.Y. Yu

Q: Could you elaborate further on the blade construction?

A: *Referring to Figure 1, we can see the stall shaft and plate insert near the root. The steel is bounded to the fiberglass box which is present for the complete span of the blade. The fiberglass box is bounded to the outside skin having a NACA 4415 profile.*

From: A.D. Garrad

Q: Do you have an estimate for the damping in the blade?

A: *No, but some stationary blade vibration tests are being done now and exponential decay will be measured to obtain an estimate of structural damping. Aerodynamic damping will not be measured.*

